Phys. Status Solidi B **248**, No. 11, 2500–2503 (2011) / **DOI** 10.1002/pssb.201100137

physica status solidi b
www.pss-b.com
basic solid state physics

Low-temperature growth of multi-walled carbon nanotubes by thermal CVD

Niina Halonen[*,1], András Sápi[2], László Nagy[2], Róbert Puskás[2], Anne-Riikka Leino[1], Jani Mäklin[1], Jarmo Kukkola[1], Geza Tóth[1], Ming-Chung Wu[3], Hsueh-Chung Liao[3], Wei-Fang Su[3], Andrey Shchukarev[4], Jyri-Pekka Mikkola[4], Ákos Kukovecz[2], Zoltán Kónya[2], and Krisztián Kordás[1,4]

[1] Microelectronics and Materials Physics Laboratories, University of Oulu, P.O. Box 4500, 90014 Oulu, Finland
[2] Department of Applied and Environmental Chemistry, University of Szeged, 6720 Szeged, Rerrich Béla tér 1, Hungary
[3] Department of Materials Science and Engineering, National Taiwan University, No. 1, Sec. 4, Roosevelt Road, Taipei 10617, Taiwan
[4] Department of Chemistry, Institute of Technical Chemistry, Chemical-Biological Center, Umeå University, 901 87 Umeå, Sweden

Received 5 May 2011, revised 20 June 2011, accepted 6 July 2011
Published online 17 August 2011

Keywords low-temperature CNT growth, thermal CVD

* Corresponding author: e-mail nhalo@ee.oulu.fi, Phone: +358-40-5901080, Fax: +358-8-5532728

Low-temperature thermal chemical vapor deposition (thermal CVD) synthesis of multi-walled carbon nanotubes (MWCNTs) was studied using a large variety of different precursor compounds. Cyclopentene oxide, tetrahydrofuran, methanol, and xylene:methanol mixture as oxygen containing heteroatomic precursors, while xylene and acetylene as conventional hydrocarbon feedstocks were applied in the experiments. The catalytic activity of Co, Fe, Ni, and their bi- as well as tri-metallic combinations were tested for the reactions. Low-temperature CNT growth occurred at 400 °C when using bi-metallic Co–Fe and tri-metallic Ni–Co–Fe catalyst (on alumina) and methanol or acetylene as precursors. In the case of monometallic catalyst nanoparticles, only Co (both on alumina and on silica) was found to be active in the low temperature growth (below 500 °C) from oxygenates such as cyclopentene oxide and methanol. The structure and composition of the achieved MWCNTs products were studied by scanning and transmission electron microscopy (SEM and TEM) as well as by Raman and X-ray photoelectron spectroscopy (XPS) and by X-ray diffraction (XRD). The successful MWCNT growth below 500 °C is promising from the point of view of integrating MWCNT materials into existing IC fabrication technologies.

1 Introduction In order to exploit the unique properties of carbon nanotubes (CNTs), we have to be able to integrate CNTs with existing materials and technologies. Direct growth of aligned CNT films on a desired substrate would be a practical, cost-effective, and elegant method but the bottleneck is the high synthesis temperature which is incompatible with many materials. For instance, in the case of IC fabrication technologies, direct CNT growth should occur below 500 °C. Typically when using thermal chemical vapor deposition (thermal CVD) or plasma enhanced chemical vapor deposition (PECVD) to produce uniform, highly graphitized, well-aligned CNT films the growth temperature should be around 600–800 °C [1–9], although there have been reports of CNT growth below 600 °C using various types of catalyst/precursor combinations. Low temperature carbon nanofiber/nanotube growth by PECVD has been accomplished on Ni [10–16], Fe or Fe–Mo [17], and $Ni_{0.67}$–$Fe_{0.33}$ [18] catalysts from mainly C_2H_2/NH_3 or CH_4/H_2 precursors. Low temperature thermal CVD grown nanotubes were synthesized from C_2H_2/NH_3 and C_2H_2 precursors on Al–Fe [19] and Co–Ti [20] layered-type catalysts combinations, respectively.

Here we report on a low-temperature MWCNT growth (below 500 °C) on mono-, bi-, and trimetallic catalyst materials by thermal CVD using acetylene as well as heteroatomic precursors (cyclopentene oxide and methanol).

2 Experimental

2.1 CNT growth on drop cast monometallic catalyst on silica Co and Fe nanoparticles (Nanostructured and Amorphous Materials, Inc.) with average particle size of 25–28 nm were dispersed in xylene (1 mg/mL) in

ultrasonic bath and immediately drop casted on Si/SiO_2 chips. After drying in ambient air, the chips were placed in a tube furnace which was then sealed, evacuated twice followed by flushing with Ar/H_2 (85%/15%) and heated to 470 °C. The carbon source (0.1 mL/min of cyclopentene oxide, methanol, xylene, xylene:methanol (vol. 1:3), or tetrahydrofuran) was introduced from an evaporation column to the reactor. The Ar/H_2 carrier feed rate was ~40 mL/min and growth time of 40 min was applied in each case.

2.2 Synthesis of mono-, bi-, and trimetallic catalysts on alumina and CNT growth Each catalyst was synthesized by wet impregnation and subsequent thermal decomposition of the corresponding metal-nitrate salts. Catalyst powders with total metal loadings of 5% by weight were applied (i.e., 5% in monometallic; 2.5% of each metal in bimetallic; and 1.67% of each metal in trimetallic catalyst). In a typical synthesis, a proper amount of nitrate salt of iron, cobalt and nickel (Sigma–Aldrich) were dissolved in ethanol and sonicated with aluminum-hydroxide/ethanol suspension for 10 min followed by the evaporation of ethanol at 60 °C in vacuum. One hundred milligrams of the as-prepared catalyst powders were pre-heated for 10 min in N_2 immediately before the CNT growth process. N_2 gas with flow rate of 100 mL/min was bubbled through a saturator containing methanol thermostated at 60 °C and the gas mixture was lead to a preheated tube furnace (300–500 °C). After an hour of synthesis time the product was allowed to cool down in N_2 gas.

Experiments with acetylene were carried out by adding 10 mL/min carbon source to the 100 mL/min N_2 carrier flow (total flow rate of 110 mL/min). Catalyst composition of 2.5–2.5–2.5% Fe–Co–Ni on alumina was applied.

2.3 Analysis of growth products Raman spectra of the samples were assessed by a Horiba Jobin-Yvon LabRAM HR800 UV–Vis μ-Raman spectroscope equipped with an Ar^+ laser (wavelength of 487.99 nm). Field emission scanning electron microscopy (FESEM, Zeiss ULTRA plus and Hitachi S4700), transmission electron microscopy (TEM, Philips CM10 and LEO 912 OMEGA, 120 kV), and high-resolution transmission electron microscopy (HR-TEM, FEI Tecnai G2 T20, 200 kV) were utilized to study morphology and structure of the nanotubes. Chemical composition was analyzed by X-ray photoelectron spectroscopy (XPS, Kratos Axis Ultra DLD, with monochromated Al Kα source, analysis area of $0.3 \times 0.7\ mm^2$, with charge neutralizer). Processing of the spectra was accomplished with the Kratos software. X-ray diffraction (XRD) (Rigaku MiniFlex II, Cu Kα source) was used for crystal structure explorations.

3 Results and discussion The synthesis produced clearly visible black deposits already at 470 °C when using Co and cyclopentene oxide whereas chips remained blank when using other catalyst nanoparticles (i.e., Fe) or precursors (methanol, xylene, xylene:methanol, tetrahydrofuran). FESEM analysis shows films of curved tangled tubular features on the substrate (Fig. 1a). The thickness of the films (not uniform) is less than a micrometer. TEM and HR-TEM (Fig. 1b–d) reveal the material consists of highly defectious multi-walled carbon nanotubes (MWCNTs) with considerable amount of amorphous deposits. Raman spectrum in Fig. 1e shows the typical D- and G-bands of sp^3 and sp^2 hybridized carbon at 1344 and 1605 cm^{-1}, respectively. According to XPS shown in Fig. 1f the majority of the deposit is graphitic carbon (carbon concentration at the sample surface is ~99.0 at.%). The asymmetric shape of C 1s peak is typical for carbon in sp^2 hybridization. The detected

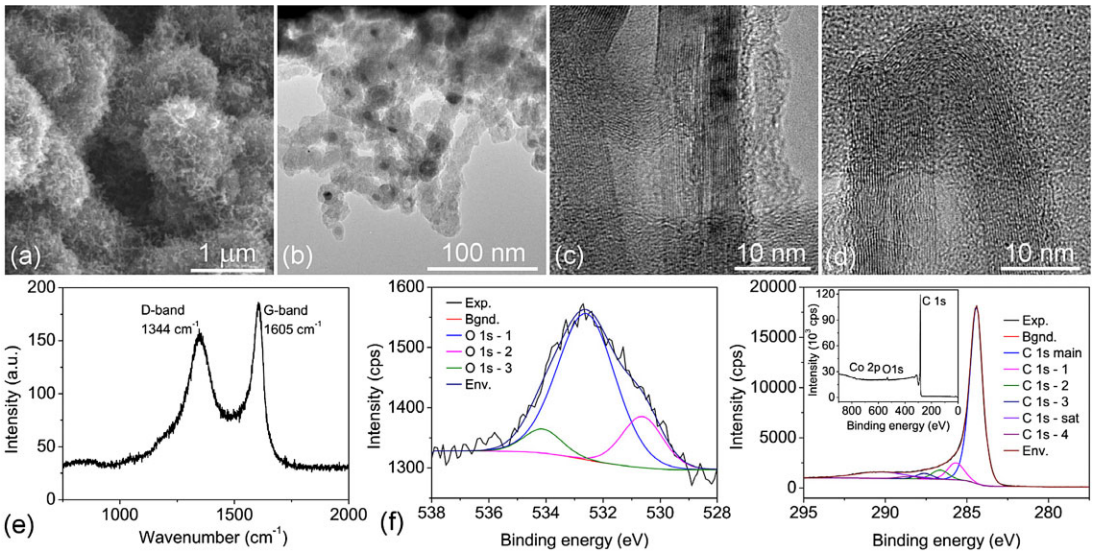

Figure 1 (online color at: www.pss-b.com) (a) FESEM, (b) TEM, and (c, d) HR-TEM images of the deposits grown on Co catalyst at 470 °C from cyclopentene oxide. (e) Raman and (f) X-ray photoelectron spectra of the nanotubes.

oxygen (∼1.0 at.%) is mainly due to oxygen containing surface functional groups [21] and traces of Co(OH)O catalyst.

In the case of monometallic catalysts synthesized on alumina nanoparticles, formation of carbonaceous deposits was not found up to 500 °C from methanol precursor. However, when applying bimetallic and trimetallic catalysts, clear appearance of carbonaceous deposits was observed already at 400 °C or below, and showed sharp increase of the deposited product with temperature (Fig. 2). The most active catalyst compositions were Fe–Co (2.5–2.5%) and Fe–Co–Ni (1.67–1.67–1.67%).

X-ray diffraction patterns shown in Fig. 3 support the gravimetric measurement data. The graphitic (002) reflection at 25.9° appears for the samples grown at or above 400 °C (Fig. 3a). Reflections measured on the 350 °C sample at ∼30.0 and 35.5° are due to the (220) and (311) planes of the $CoFe_2O_4$ phase (pdf# 011121), while the broadened peaks at 37.0 and 43.0° are due to the reflections from the (111) and (200) planes of NiO nanoparticles (pdf# 780643) (Fig. 3b). The appearance of reflection around 44° suggests the oxide phases are reduced into metallic forms of the catalysts assigned to Ni (111), Fe (110), and Co (002) planes (pdf# 040850; 060696; 050727) at or above 350 °C. The vanishing 14.4, 28.1, 38.4, and 49.1° reflections at higher temperatures are due to interlayer dehydratation and phase transition of boehmite (γ-AlO(OH)) into γ-Al_2O_3.

Scanning electron microscopy and TEM analyses show only amorphous carbon on the sample synthesized at 350 °C. CNTs appear in the samples grown at temperatures at or above 400 °C (Fig. 4).

It is worth mentioning, that preliminary experiments with acetylene have been successful to grow MWCNTs at low-temperatures. Already at 400 °C, nanotubes emerged from the Fe–Co–Ni trimetallic catalyst (2.5–2.5–2.5%).

It is a generally accepted view for nanotube growth, that the carbon precursor has to decompose to carbon atoms or to a few atomic clusters before those are adsorbed on or dissolved in the catalyst nanoparticles. When cracking hydrocarbons, the first bond cleavage is the most energy demanding step. Since the bonds in hydrocarbons are very energetic (C–C, ∼350 kJ/mol and C–H, ∼410 kJ/mol) [22] cracking can take place only at high temperatures. Once radicals have formed, the subsequent reaction steps towards the decomposition of the molecule should take place [23]. Accordingly, having low energy bonds such as the C–O epoxide (∼280 kJ/mol) in cyclopentene oxide [24] is expected to enhance radical formation allowing the precursor to decompose at lower temperatures than with saturated and aromatic hydrocarbons. In the case of methanol, the weakest bond is the C–OH (385 kJ/mol) [25] which can explain why xylene:methanol mixture was not a suitable precursor at such a low temperature using the same catalyst.

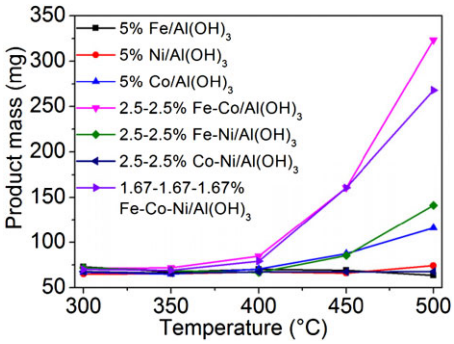

Figure 2 (online color at: www.pss-b.com) Mass of the products as a function of catalyst composition and growth temperature after 1 h growth.

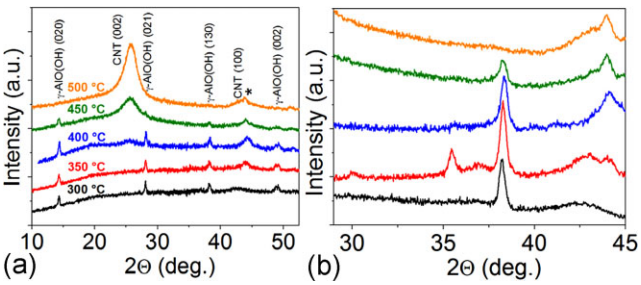

Figure 3 (online color at: www.pss-b.com) (a) XRD patterns of growth products on Fe–Co–Ni trimetallic catalysts at different synthesis temperature. Symbol * at $2\Theta \sim 44°$ denotes reflections that may be assigned to Ni (111), Fe (110), and Co (002) planes (pdf# 040850; 060696; 050727). (b) Higher resolution diffraction pattern for $29° < 2\Theta < 45°$ angles showing the gradual transformation of boehmite into alumina as well as the reduction of oxides to metals.

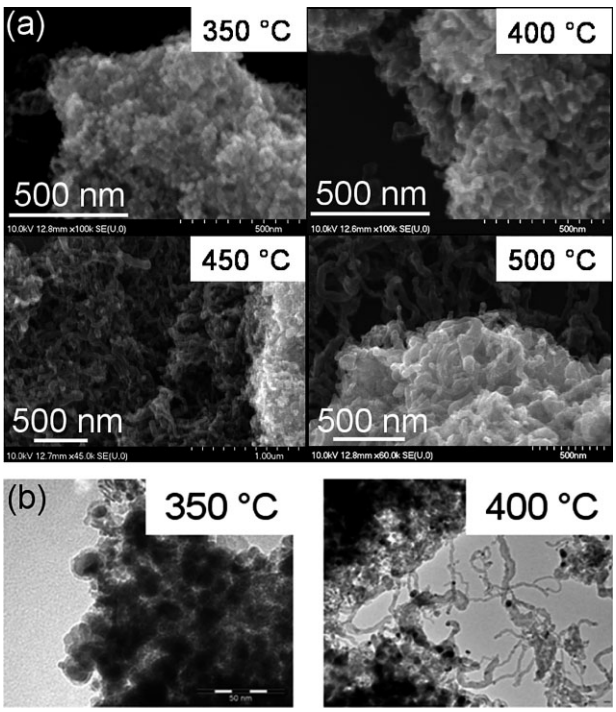

Figure 4 (a) SEM and (b) TEM images of deposits grown on Fe–Co–Ni trimetallic catalysts between 300 and 500 °C. Nanotubes clearly appear on the samples synthesized at 400 °C and above.

In the case of bi- and trimetallic catalysts, the particular function of metals is not well understood. The different carbon solubilities as well as surface/bulk diffusion rates on/in the metals can provide a broader parameter window for both nucleation and growth [29]. On the other hand, the Fe–Co–Ni based mixed oxide catalyst/Al_2O_3 support may enhance dehydration of the methanol precursor allowing lower decomposition temperatures compared to single metal catalyst systems [30]. Several groups have shown earlier, that CNT growth rate on bimetallic catalyst compositions can be considerably higher than on the corresponding individual metals [26–28]. Our results also support these findings for methanol precursor. Preliminary experiments with acetylene show also good activity on the trimetallic catalyst, however further studies are required to compare the growth rates with those on mono- or bimetallic catalyst materials. Anyhow, the week π bonds between the carbon atoms in acetylene may be responsible for the reactivity of this precursor.

Apart from the easy decomposition of oxygenates, a further possible advantage of using such precursors is the continuous supply of oxygen which can help keeping the catalyst surface clean similar to that found for precursors with added water [31, 32].

4 Summary We have grown MWCNTs at low temperatures (below 500 °C) by thermal CVD on Co catalyst from cyclopentene oxide, on various bi- and trimetallic catalyst combinations of Fe, Co, and Ni from methanol, and on trimetallic Fe–Co–Ni catalyst from acetylene. The results suggest that low energy covalent bonds in precursor molecules can initiate decomposition of the source and allow CNTs growth at lower temperatures than from saturated hydrocarbons.

Acknowledgements N. H. acknowledges the postgraduate student post received from the NGS-Nano. J. K. acknowledges the Infotech Oulu, the Riitta and Jorma J. Takanen foundation and the Emil Aaltonen foundation for financial support. G. T. thanks the researcher post received from the Academy of Finland. The work is supported by the projects ThemaCNT (EU FP7), RoCaNaMe (Academy of Finland), TÁMOP-4.2.1/B-09/1/KONV-2010-0005, the Hungarian Scientific Research Fund (project number: OTKA NNF2 85899), and Bio4Energy program.

References

[1] K. Mukhopadhyay, A. Koshio, T. Sugai, N. Tanaka, H. Shinohara, Z. Konya, and J. B. Nagy, Chem. Phys. Lett. **303**, 117 (1999).
[2] B. Q. Wei, R. Vajtai, Y. Jung, J. Ward, R. Zhang, G. Ramanath, and P. M. Ajayan, Nature **416**, 495 (2002).
[3] Y. J. Jung, B. Wei, R. Vajtai, P. M. Ajayan, Y. Homma, K. Prabhakaran, and T. Ogino, Nano Lett. **3**(4), 561 (2003).
[4] G. Meng, Y. J. Jung, A. Cao, R. Vajtai, and P. M. Ajayan, Proc. Natl. Acad. Sci. USA **102**(20), 7074 (2005).
[5] K. Mizuno, K. Hata, T. Saito, S. Ohsima, M. Yumura, and S. Iijima, J. Phys. Chem. B **109**, 2632 (2005).
[6] J. K. Radhakrishnan, P. S. Pandian, V. C. Padaki, H. Bhuan, K. U. B. Rao, J. Xie, J. K. Abraham, and V. K. Varadan, Appl. Surf. Sci. **255**, 6325 (2009).
[7] J. Jiang, T. Feng, X. Cheng, L. Dai, G. Cao, B. Jiang, X. Wang, X. Liu, and S. Zou, Nucl. Instrum. Methods Phys. Res. B **244**, 327 (2006).
[8] J. Jiang, T. Feng, J. H. Zhang, X. H. Cheng, G. B. Chao, B. Y. Jiang, Y. J. Wang, X. Wang, X. H. Liu, and S. C. Zou, Appl. Surf. Sci. **252**, 2938 (2006).
[9] N. Halonen, K. Kordás, G. Tóth, T. Mustonen, J. Mäklin, J. Vähäkangas, P. M. Ajayan, and R. Vajtai, J. Phys. Chem. C **112**(17), 6723 (2008).
[10] S. Hofmann, B. Kleinsorge, C. Ducati, A. C. Ferrari, and J. Robertson, Diamond Relat. Mater. **13**, 1171 (2004).
[11] S. Hofmann, C. Ducati, B. Kleinsorge, and J. Robertson, Appl. Phys. Lett. **83**(22), 4661 (2003).
[12] K. Y. Lee, M. Katayama, S. Honda, T. Kuzuoka, T. Miyake, Y. Terao, J.-G. Lee, H. Mori, T. Hirao, and K. Oura, Jpn. J. Appl. Phys. **42**, L804 (2003).
[13] H. S. Kang, H. J. Yoon, C. O. Kim, J. P. Hong, I. T. Han, S. N. Cha, B. K. Song, J. E. Jung, N. S. Lee, and J. M. Kim, Chem. Phys. Lett. **349**, 196 (2001).
[14] S.-C. Chang, T.-C. Lin, T.-S. Li, and S.-H. Huang, Microelectron. J. **39**, 1572 (2008).
[15] N. Chiodarelli, Y. Li, D. J. Cott, S. Mertens, N. Peys, M. Heyns, S. De Gendt, G. Groeseneken, and P. M. Vereecken, Microelectron. Eng. **88**, 837 (2011).
[16] M. Dubosc, S. Casimirius, M.-P. Besland, C. Cardinaud, A. Granier, J.-L. Duvail, A. Gohier, T. Minéa, V. Arnal, and J. Torres, Microelectron. Eng. **84**, 2501 (2007).
[17] E. J. Bae, Y.-S. Min, D. Kang, J.-H. Ko, and W. Park, Chem. Mater. **17**(20), 5141 (2005).
[18] W.-H. Chiang and R. M. Sankaran, Adv. Mater. **20**, 4857 (2008).
[19] M. Cantoro, S. Hofmann, S. Pisana, V. Scardaci, A. Parvez, C. Ducati, A. C. Ferrari, A. M. Blackburn, K.-Y. Wang, and J. Robertson, Nano Lett. **6**, (6), 1107 (2006).
[20] T.-Y. Tsai, N.-H. Tai, K. C. Chen, S. H. Lee, L. H. Chan, and Y. Y. Chang, Diamond Relat. Mater. **18**, 307 (2009).
[21] M. Phaner-Goutorbe, A. Sartre, and L. Porte, Microsc. Microanal. Microstruct. **5**, 283 (1994).
[22] P. Atkins and J. de Paula, Atkins' Physical Chemistry, eighth edition (Oxford University Press, Italy, 2006), p. 1012.
[23] Y. Xiao, J. M. Longo, G. B. Hieshima, and R. J. Hill, Ind. Eng. Chem. Res. **36**, 4033 (1997).
[24] G. Glockler, J. Phys. Chem. **62**(9), 1049 (1958).
[25] D. R. Lide, CRC Handbook of Chemistry and Physics, 72nd edition (CRC Press, Boca Raton, USA, 1991).
[26] N. Nagaraju, A. Fonseca, Z. Konya, and J. B. Nagy, J. Mol. Catal. A **181**, 57 (2002).
[27] Á. Kukovecz, Z. Kónya, N. Nagaraju, I. Willems, A. Tamási, A. Fonseca, J. B. Nagy, and I. Kiricsi, Phys. Chem. Chem. Phys. **2**, 3071 (2000).
[28] A. M. Cassell, J. A. Raymakers, J. Kong, and H. Dai, J. Phys. Chem. B **103**, 6484 (1999).
[29] W. Q. Deng, X. Xu, and W. A. Goddard III, Nano Lett. **4**, 2331 (2004).
[30] T. Zaki, J. Colloid Interface Sci. **284**, 606 (2005).
[31] K. Hata, D. N. Futaba, K. Mizuno, T. Namai, M. Yumura, and S. Iijima, Science **306**, 1362 (2004).
[32] D. N. Futaba, K. Hata, T. Yamada, K. Mizuno, M. Yumura, and S. Iijima, Phys. Rev. Lett. **95**, 056104 (2005).